

Numerical and Experimental Analysis of Thermal Performance in Triple-Glazed Low-E Windows for Iraqi Weather

Mina A. Nsaif^{1*} , Jalal M. Jalil² , Mounir Baccar¹ 

¹Advanced Fluid Dynamics, Energetics and Environment Laboratory, Department of Mechanical Engineering, National School of Engineers of Sfax, University of Sfax, Tunisia

²Electromechanical Engineering Department, University of Technology, Baghdad, Iraq

*Email: mina-abdulkareem-nsaif.alshareefi@enis.tn

Article Info	Abstract
<p>Received 22/07/2024</p> <p>Revised 27/04/2025</p> <p>Accepted 18/05/2025</p>	<p>Low-emissivity (low-e) glass is a highly efficient material capable of adapting its thermal and optical properties in response to temperature fluctuations without consuming additional Energy. This makes it an ideal choice for passive building envelopes, particularly in climates with extreme temperatures. In this study, the thermal efficiency of triple glazed windows incorporating low-e glass was experimentally evaluated under the harsh summer conditions of Iraq. Specifically, a conventional triple-glazed window (TG1) with air-filled gaps was compared to a modified version (TG2) featuring low-e glass on the outer pane, also with air in both gaps. The research findings revealed that when solar radiation peaked at 650 W/m² around midday in July, the internal surface temperatures of TG1 and TG2 were 36.4°C and 32.4°C, respectively. The temperature reduction observed in TG2, amounting to 4°C (10.9%), highlights the significant thermal advantage the low-e glass provides, making it a superior option for enhancing energy efficiency in buildings.</p>
<p>Keywords: Improve thermal performance, Internal surface temperature, Low-e glass, Thermal Performance, Triple-glazed window.</p>	

1. Introduction

Building envelopes are necessary for balancing human comfort with the environmental effects caused by buildings by acting as the boundary between interior and outdoor spaces. An adaptive facade can selectively regulate the transmission, filtering, or absorption of heat, mass transfer, and light between the interior and outer environments. This presents an opportunity to enhance inner environmental quality while simultaneously reducing the energy dissipation of rooms. Kamalisarvestani et al. [1] used thermochromic windows, which change color and optical properties with temperature. This study examines thermochromic window performance, materials, coatings, and energy modeling.

Additionally, the study examines the impacts of doping vanadium dioxide (VO₂) coatings with tungsten, fluorine, and gold nanoparticles. Both hybrid chemical vapor deposition and physical vapor deposition are explained. Dopants and methods affect the MST and critical temperature differently. Changes in visible and infrared transmission and reflectance measure the

performance of chromogenic smart windows. Khaled and Berardi [2] observed that passive coatings similar to thermochromic and photochromic coatings are more suitable and easily reachable for glazing applications. The work also found that thermochromic coatings using vanadium dioxide (VO₂) are more advanced. Thermochromic glazing tests are advancing in two ways. One technique involves identifying the best optical qualities for various conditions through numerical simulation or an outdoor experiment. Long and Ye [3] investigated the performance of (VO₂) intelligent glazing by evaluating the energy-saving equivalent and the energy-saving index. The investigators find the optimal characteristics of the substance for effective smart temperature modulation indoors. Arnesano et al. [4] suggested an approach for styling the thermochromic glazing and determined the optimal thermochromic optical response to minimize energy waste in the building. Hong et al. [5] investigated the most effective thermochromic glazing to reduce energy usage and increase daylight access. The opposing approach involves increasing the optical characteristics and adjusting the phase transition temperature using a creative process. Liu et al. [6] utilized anti-

reflective covering to enhance the UV light-blocking capability of thermochromic glazing containing different VO₂. Salamati et al. [7] created TiO₂W-VO₂ thermochromic glazing with notable modulation ability at near-infrared wavelengths. Gagaoudakis et al. [8] investigated the best ways for depositing VO₂ so that it could form a thermochromic monoclinic phase. They did this for a range of substrates and thicknesses, and the results showed how these factors affected the critical transition temperature and light transmission. In addition, PCM utilization is a passive adaptive material capable of increasing the thermal mass of building envelopes through latent heat. Its use in the transparent or glassy parts of building envelopes has been researched through numerical and experimental methods.

Huang et al. [9] analyzed the optical characteristics of online Low-E glass. The calculation relating transmittance and optical constants was accepted using the central methods and Drude theory in thin-film optics. The optical properties of the functional coating of Low-E glass were determined by fitting the regular transmission spectrum with a theoretical formula to get the optical constants. The Burstein-Moss theory was applied to study the free-carrier mass in the functional layer. The predicted outcomes align with the experimental findings.

Yuxuan et al. [10] created and measured thermochromic coatings in five colors. In Shanghai, thermochromic coatings had a lower average daily surface temperature than the common coating during cooling. They maintained a higher average daily surface temperature than the cool coating during heating. The annual energy consumption results demonstrated that thermochromic coatings could prevent the high heating loads associated with cool coatings. Thermochromic coatings could cut the office building's annual energy consumption by 4.28–5.02 kWh/m² compared to the ordinary coat and 0.73–1.47 kWh/m² compared to the cool coat. Tao et al. [11] investigated normal clear glass and low-e glazing within a naturally ventilated double-skin façade (NVDSF). The investigation examined the effect of spectral optical characteristics, ambient conditions, and configurations on performance. The findings showed an important increase, with a 13% rise in ventilation rate when low-e glass was substituted for clear glass. The spectral optical characteristics of low-e glazing affected the ventilation efficiency, where increased absorptivity was found to be more beneficial for natural ventilation.

Also, researchers have used phase change material as an insulating material in triple and double-glazing systems. Wang et al. [12] proposed a double-glazed unit design that utilizes phase-change material with solar control glass. They evaluated its thermal efficiency through numerical simulations in sunny and gloomy circumstances during the summer in northern China. An increase in the glass absorption coefficient increased the melting of PCM but negatively impacted thermal comfort, perhaps causing overheating on bright days. The energy savings rate was 14.25% with a glass absorption coefficient of 160 m² on sunny days, and it improved to 41.53% with a glass refractive index of 3. Baldinelli [13] optimized winter and summer energy performance. Using central Italy's climate, they developed a south-facing façade model. Ray tracing and various interface reflections were used to model the solar radiation route. Simulations were validated using data from a comparable

investigation. Despite shading regulations, the planned façade agreement allowed adequate solar heat gain in winter. Jalil and Salih [14] used a numerical study to assess how variable PCM's thermal properties influence double-glazed windows. The study observed that increasing the thermal capacity, PCM thickness, latent heat, and density of a phase-change material accelerated the temperature drop and reduced the temperature decline factor of the double-glazed window, and changes in paraffin wax increased window unit efficiency proportionally.

Jalil and Salih [15] tested the thermal efficiency of a double-glazed window integrated with paraffin wax using theoretical and experimental methods. The study aimed to lower summer cooling needs, increase window thermal resistance, and control temperature fluctuations. The results indicated significantly lower temperatures for double-glazed windows than for single-glazed ones. Temperature decreases of 8 °C for the ground floor, 6 °C for the first floor, and 5 °C for the ceiling were observed.

Gowreesunker et al. [16] conducted a study using the T-history method to test and figure out how well a PCM-integrated double-glazing window worked. The PCM absorption coefficients, scattering, extinction, and absorption were expressed and used for the numerical CFD study. The study results show that including PCM enhances the thermal inertia of the glazing through the phase transition, but may result in overheating once the PCM melts. Yang et al. [17] evaluated double-glazed windows filled with Al₂O₃-CuO hybrid Nano-PCMs, finding that increasing CuO enhances energy savings and economy, while Al₂O₃ improves thermal comfort and lighting. The optimal CuO: Al₂O₃ ratio is 4:6.

Zhang et al. [18] enhanced a building's thermal inertia and managed peak loads using PCM. However, traditional PCM windows face energy inefficiency and overheating risks. A rotating dynamic PCM window (DPCMW) was developed to address this, featuring a PCM layer and a vacuum glass layer. The DPCMW adjusts these layers to control heat flux, improving energy efficiency. Compared to static PCM windows (SPCMW), DPCMW reduces heating and cooling loads by 12.40% in winter and 93.79% in summer, respectively, lowering the annual building load by 28.70%. Optimal PCM parameters were identified for maximum efficiency.

Nur-E-Alam et al. [19] studied glass components that are laminated and coated with low-e layers, particularly those with tailored double-silver low-E coatings, that offer enhanced energy savings and durability for window retrofits. This study explores the design and fabrication of high-stability solar control low-E coatings on 3 mm glass substrates, using RF magnetron sputtering and lamination with transparent epoxy and PVB. Results show these coatings, shielded by a transparent glass layer, slightly reduce optical transmission by 8–10%, meanwhile maintaining low thermal emissivity. This research could significantly contribute to sustainable building practices and reduced energy consumption if industrialized.

Bianco et al. [20], [21] conducted a comprehensive outdoor test in the cold and summer months to assess the effectiveness of a triple glazing unit comprising PCM and a thermotropic glass

pane. The study also examined how the PCM layer's position under good weather conditions affects thermal performance. Several studies have examined the details of phase change material and thermochromic glazing individually. However, few have investigated the overall thermal efficiency of a glazing component that combines both approaches.

Kuřakowski et al. [22] found that the optimal design for triple-glazed units with PCM in the cavity has a PCM layer with a 25 °C melting temperature. Simulation results, validated by experiments, showed varying optimal PCM thicknesses between 5 and 20 mm, determined using the Weighted Sum and Fuzzy Sets methods. For thermal impact, Dheyab and Al-Jethelah [23] tested an absorber-finned heat exchanger-thermal storage unit in a solar air heater. RT42 and RT50 PCMs are used in two solar air warmers. Every PCM fills the thermal storage of the SAH. In thermal storage, air was forced through a finned heat exchanger. There were two setups attempted. The SAHs were divided in the initial setup. The RT50 and RT42 SAHs were linked in sequence in the second configuration. The greatest temperature that RT50 attained in the separation arrangement was 59 °C. Forced air was heated by the RT50 solar air heater in series till five in the morning the next day.

Abbas and Azat [24] tested the Rayleigh number and passive solar mass flow rate using Trombe walls composed of industrial wax as PCM. All but the south wall of a test rig consisting of PVC sandwich panels for cubicles was produced. Trombe wall, then covered in a 6 mm thick layer of clear glass. Six air gap channel widths were used in the six winter trials conducted in Kirkuk City: 10, 15, 20, 25, 30, and 35 cm. According to experimental results, the mass flow rate is directly proportional to channel width and inversely proportional to Rayleigh number. At 30 cm depth, the maximum efficiency was 2.45 times greater than at 10 cm.

Ismail and Henriquez [25], [26], and Ismail et al. [27] studied the energy consumption and heat transfer efficiency of buildings with phase change materials (PCMs) using both numerical and experimental methods. According to their research, PCMs can reduce heat transmission and selectively block thermal radiation. Therefore, in an independent investigation, it was discovered that windows with PCM-filled glazing units were more thermally efficient than windows with air-filled glazing units.

Sorooshnia et al. [28] studied the PCM used for foam in window shutters; solar radiation entering indoor spaces is reduced. PCM shutters are more thermally efficient than foam shutters, decreasing heat absorption through windows by up to 23.29% during regular hours. Goia et al. [29]-[32] indicated that transparent PCM-filled materials can store solar Energy, enhancing the thermal inertia of glazing systems and smoothing out peak heat flow values.

Koshlak et al. [33] demonstrated that electrically heated low-emissivity coatings on double-glazed windows can direct 83–85% of heat indoors, enhancing thermal comfort and serving as an emergency heating system during extreme cold. A recent study by Basok et al. [34] used comprehensive CFD and experimental analysis to evaluate the thermal performance of electrically heated windows. Findings showed that such

windows could reduce room energy consumption by 10–12% through improved heat transfer processes, demonstrating the potential of advanced glazing technologies for enhancing energy efficiency and indoor comfort. Research analyzing the deflection and stress in triple-glazed IGUs positioned horizontally has highlighted the impact of climatic loads, including temperature changes and atmospheric pressure. The study found that while horizontal placement mitigates the effects of pressure drop and wind suction, extreme temperature shifts pose a risk of excessive deflection [35].

This study experimentally investigated two systems of triple-glazed windows filled with air and the effect of integrated low-e glass in the external layer glass of the triple-glazed windows to improve the thermal performance in the July months under the Iraqi environment.

TG1: A standard triple-glazed window with air in both gaps.

TG2: A triple-glazed window in which the outer glass is a low-e and air is in both the gaps.

2. Experimental Work

In Fig. 1 (a, b), the structural comparison between the two window types indicates that the test room includes two TGs, windows with three glass panels separated by two gaps to minimize thermal conduction. To reduce heat transfer, the windows are securely fastened to the frame and spaced apart with spacers.

Two types of triple-glazed windows were supposed to be used for the experiment, and Table 1 shows the construction details of the evaluated glazing systems.

The dimensions of these two types of windows were 41 cm in length and 41 cm in width, with a 2 cm gap and a 6 mm glass thickness. Halogen lamps were used in the experiment to simulate solar radiation.

The heat transfer in the triple-glazing system involves the external glass, cavity layer, and internal glass. Fig. 2 illustrates the test room model, measuring (1.5 x 1.5 x 1.5) meters, constructed with 0.06-meter-thick PVC sandwich panels for the walls and roof. A refrigerator was included in the setup to stabilize the ambient temperature in the test room, countering heat buildup from radiation. Table 2 also shows the glass's properties.

2.1 Temperature Measurement

2.1.1 Thermocouples

Type-K thermocouples were used to determine the temperature distribution across each triple-glazed window as shown in Fig. 3. Four thermocouples were positioned on each window: on the outer surface, within the first and second air gaps, and on the inner surface, as shown in Fig. 4. Each thermocouple was connected to a temperature data logger located outside the room to capture temperature variations effectively across the window assembly.

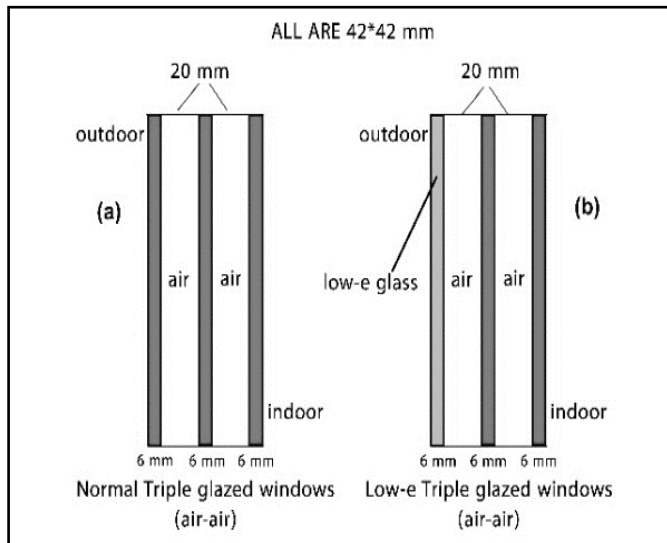


Figure 1. Structure of the windows: (a) TG1, (b) TG2.

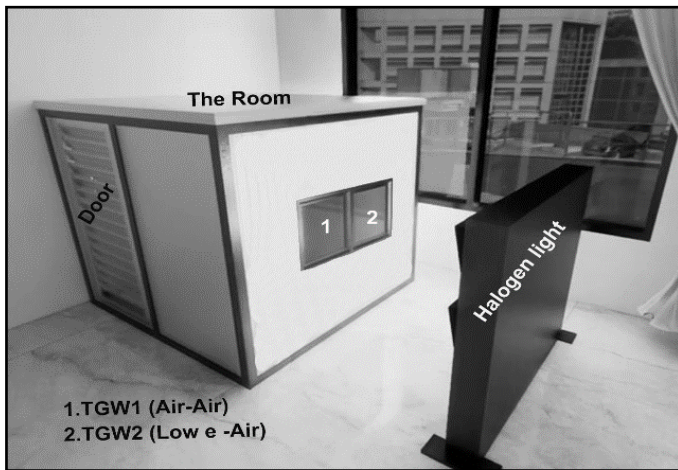


Figure 2. Two triple-glazed window models (TG1 and TG2).

Table 1. Glazing systems construction details

Type	1 st layer (outside)	Gap (20mm)	2 nd layer	Gap (20mm)	3 rd layer (inside)
TG1	glass 6 mm	air	glass 6 mm	air	glass 6 mm
TG2	low-e glass 6 mm	air	6 mm	air	glass 6 mm

2.2.2 Thermometer device

The temperatures have been measured using the HT-9815 thermometer (Fig. 5), which has four channels to connect thermocouple probes. These probes were placed in the room, on the inside and outside surfaces of the triple-glazed windows,

and within each gap between the glass layers for both windows. All data was manually logged.

Table 2. Displays the Glass’s Physical Properties [36]

Glazing					
Thickness (m)	Solar transmittance	Solar reflectance (front side)	Solar reflectance (back side)	Emissivity (front side)	Emissivity (back side)
0.006	0.804	0.074	0.074	0.84	0.84

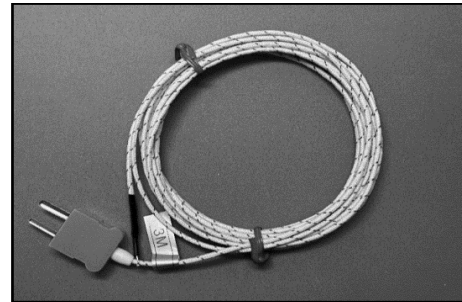


Figure 3. Sensor K-type Thermocouple.

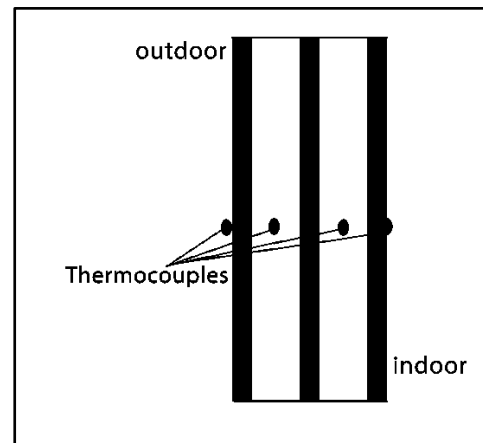


Figure 4. Insulated Thermocouples Location in Triple-Glazed Window Layers

2.2.3 Solar power meter

To measure radiation from halogen lamps hitting the surface of four triple-glazed windows, a digital LCD solar power meter SM20-SOLAR was used, as shown in Fig. 6. The device responds within 1 second and can measure radiation intensity ranging from 0.1 to 2000 W/m². Detailed specifications of the equipment are provided in Table 3.

2.3 Experimental Procedure (Steps)

Since each triple-glazed window receives the same amount of solar radiation, TG1 is a triple-glazed unit with air in both gaps, and TG2 is a triple-glazed unit in which the outer glass is a low-e and air in both gaps. After that, ensure that.

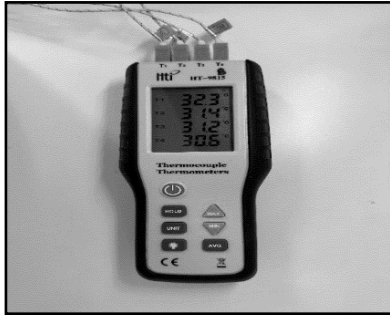


Figure 5. Thermometer.

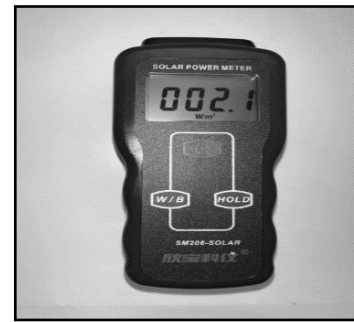


Figure 6. Solar Power Meter.

Table 3. Specifications of the measurement equipment.

Specification	Device	Type	Scope	Validity
Solar Irradiance	Solar meter	SM20-SOLAR	0.1 to 2000 W/m ²	± 4.8%
Temp.	Thermometer	HT-9825	-100 to 1350 °C	± 0.14%
	Thermocouple	Type-K	-100 to 1310 °C	± 0.38%

The source of power remains stable, with no voltage fluctuations, as this directly affects the intensity of the halogen lamps. The testing period spans from 6:00 to 18:00.

Then, the next steps would follow sequentially.

1. Verify that the thermometer is securely linked with all thermocouple probes.
2. Link the lamps to the dimmer control.
3. Confirm that the refrigeration device is functioning correctly.

These steps are applied to each triple-glazed window, as shown in Fig. 7.

3. Numerical Formulations

The numerical analysis used a three-dimensional transient model to simulate heat transfer through the triple-glazed windows. The finite volume method (FVM) discretized the partial differential equations governing conduction and convection across the glass and air layers. Energy balance equations were solved iteratively with time-stepping to capture temperature changes, and boundary conditions, such as solar radiation at 650 W/m², were applied to reflect real conditions. The model was validated by comparing results with experimental data from July, ensuring accurate temperature distribution predictions for both standard and low-e glass configurations.

The utilization of partial differential equations has been widespread in comprehending and forecasting the thermal characteristics of diverse systems. Window systems are critical to reducing energy consumption and preserving the best indoor thermal comfort in building physics and architecture. Compared to other TG, the test room's two types of TG with

two cavities provide better thermal insulation. By using effective insulation, the TG system reduces energy loss from its side and bottom windows.

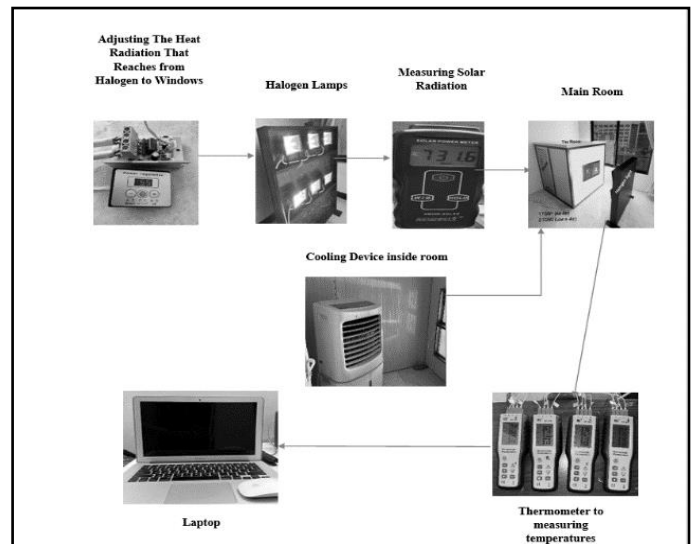


Figure 7. Experimental Procedure.

The underlying assumption made in the numerical solution is:

1. All analyses are transient and consider three dimensions.
2. All air properties are constant.
3. The effects of body force, buoyancy, and dissipation energy have been neglected.
4. All material properties were calculated using the average temperature during testing.

3.1 Thermal Analysis Framework

A three-dimensional transient model is used to analyze the triple-glazed windows, as shown in Fig. 8. To forecast multiple elements that could affect the window's thermal performance under varied climatic circumstances, a thorough thermal system simulation is essential. Conduction and convection within the triple-glazed windows' multilayered construction are easier to grasp by this model. It uses tiny, six-faced elements, which stand for the top, bottom, west, north, and east sides, within a control volume to create an energy balance. Based on this methodology. According to this method, heat entering and exiting the window system equals zero, or a net zero.

$$\sum q_{in \text{ all face}} - \sum q_{out \text{ all face}} = q_{storage} \quad (1)$$

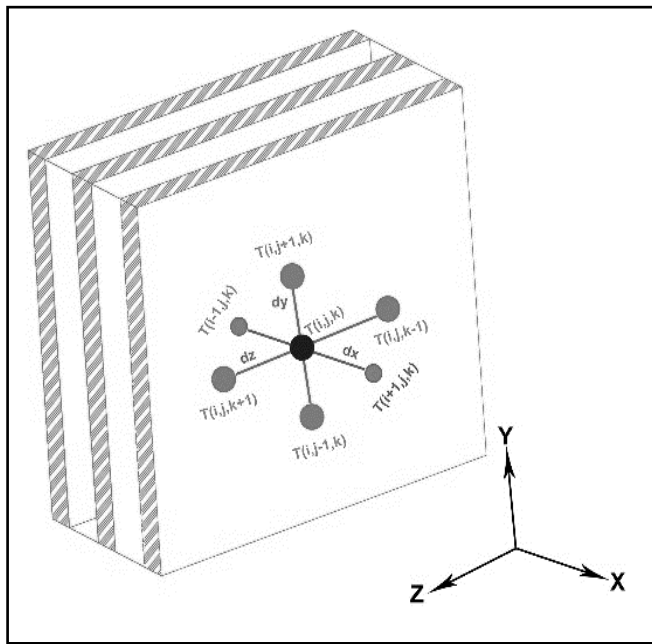


Figure 8. Three-Dimensional Node Configuration for TG

3.1.1 Triple glazed window (Air-Air) (TG1)

Enthalpy will be calculated using the energy equation across all nodes in three dimensions for glass.

$$ae = aw = \frac{kg * dt}{dg * dx^2} \quad (2)$$

$$as = an = \frac{kg * dt}{dg * dy^2} \quad (3)$$

$$at = ab = \frac{kg * dt}{dg * dz^2} \quad (4)$$

$$\begin{aligned} enew(k, i, j) = & asT(i, j - 1, k) + aeT(k, i + 1, j) \\ & + abT(i, j, k - 1) + anT(i, j + 1, k) \\ & + atT(k + 1, i, j,) + awT(i - 1, j, k) \\ & - (as + an + aw + ae + ab + at) \\ & * T(i, j, k) + eold(i, j, k) \quad (5) \end{aligned}$$

3.2 Validation of Numerical Results

Fig. 9 compares experimental and numerical results regarding temperature variations on the internal surface of two different types of triple-glazed windows. The correlation between these numerical and experimental outcomes was considered satisfactory.

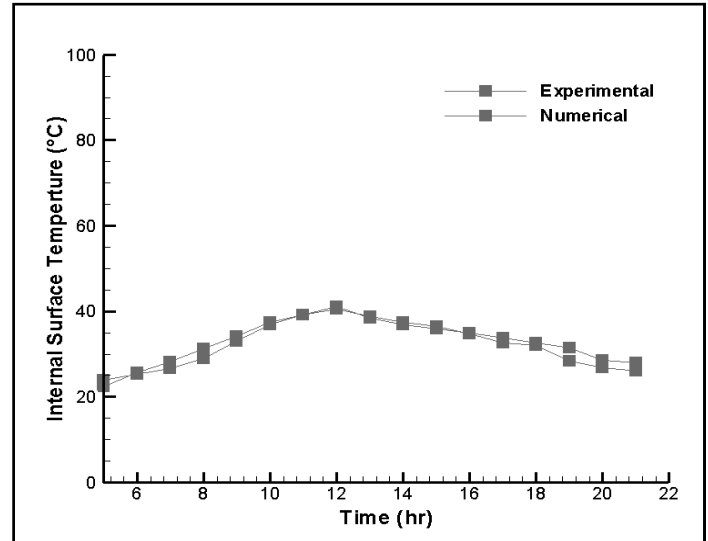


Figure 9. Comparison of experimental results with numerical data of the internal surface for validation of the temperature of the window in July of TG1

4. Results and Discussion

The study aimed to experimentally assess the effects of incorporating low-e glass as an insulator in triple-glazed windows. Under constant conditions, the experimental measures were conducted all month long, but particularly in July 2023. These experiments were conducted over several days to guarantee the accuracy of the results. Temperature data and radiation levels were recorded every 60 minutes during the experiments.

4.1 Experimental Temperature Results

Fig. 10 shows the observed patterns of solar radiation during the experiment. In July 2023, at 12:00, the maximum solar radiation measured was 650 W/m².

Fig. 11 shows the TG's variation in the external surface temperature. The figure shows a decrease in the external temperature of TG2 compared to TG1 during the day, from 6:00 to 18:00, because Low-E glass is an efficient insulator in buildings and limits the passage of heat through windows while letting visible light through.

Fig. 12 and Fig. 13 display the temperature trends of the outer and inner gaps in the two TG configurations over the July timetable. Between 6:00 and 18:00, the maximum temperatures of TG1 and TG2 in the exterior gap were 49 and 44 °C, respectively. Additionally, two windows' inner gaps had peak temperatures of 43 and 36.8 °C. The interior temperatures of the two kinds of windows with glazing (TG1 and TG2) are shown

in Fig. 14. For a triple-pane window with standard glass (TG1), the highest glass temperature at maximum sunlight 650 W/m^2 was recorded at $36.4 \text{ }^\circ\text{C}$ at 12:00. However, for a triple-pane window with low-e glass (TG2), it was only $32.4 \text{ }^\circ\text{C}$.

Both glass types warmed steadily from 6:00 a.m. to midday, then cooled toward evening. This follows the sun's daily cycle, where sunlight is strongest around noon. However, the low-E glass heated up more slowly than regular glass. This suggests that while low-E glass blocks heat from entering, it also holds onto heat longer once absorbed. As a result, windows with low-E glass stayed about 4°C cooler compared to the standard glass (TG1).

These findings suggest that the triple-glazed window with low-e glass (TG2) is more efficient in minimizing heat gain than the regular glass (TG1). The lower peak temperature observed on the internal surface of TG2 suggests that the low-e glass effectively blocks infrared radiation. This reduces the heat transfer to indoor surfaces, minimizing the thermal load on spaces with low-e glazing. In comparison, the highest inner surface temperature of the TG in Li et al. [37] was 36.5°C . In contrast, in this research, when using low-emissivity glass in the triple-glazed configuration, the highest internal surface temperature was significantly reduced to 32.4°C , representing an improvement of approximately 11%.

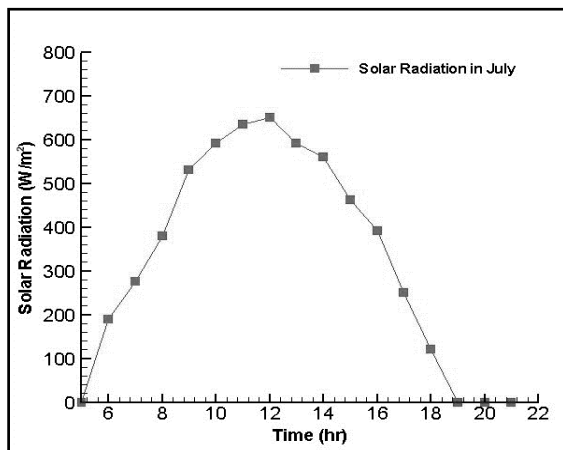


Figure 10. Daytime solar radiation intensity in July 2023.

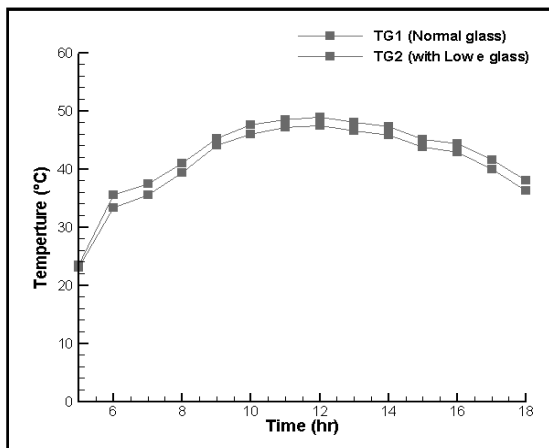


Figure 11. Daily external surface temperatures of standard vs. low-e triple-glazed windows in July 2023.

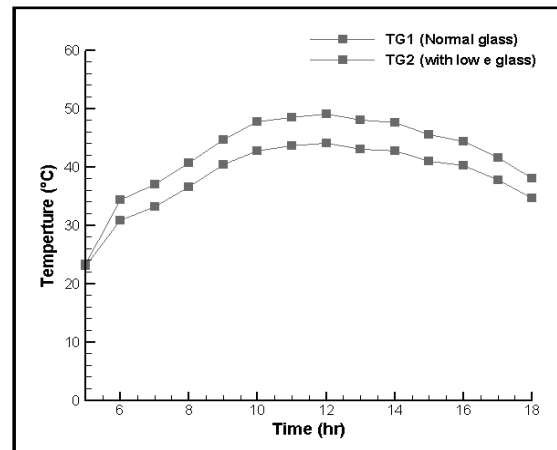


Figure 12. Daily external cavity temperatures of standard vs. low-e triple-glazed windows in July 2023.

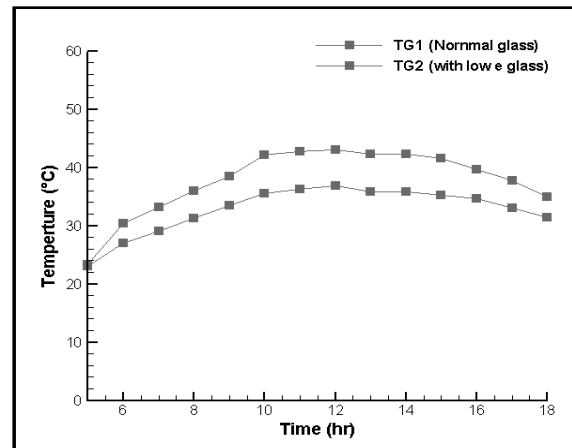


Figure 13. Daily internal cavity temperatures of standard vs. low-e triple-glazed windows in July 2023.

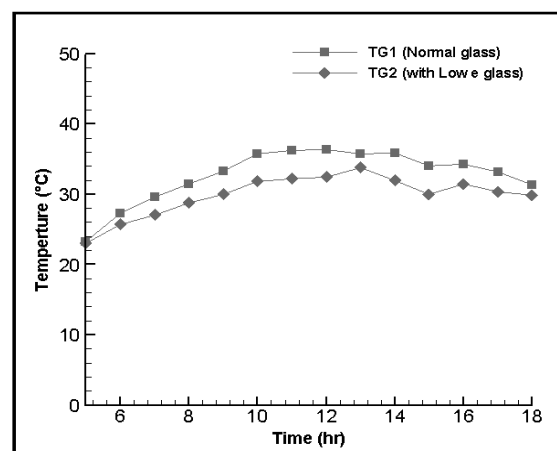


Figure 14. Daily internal surface temperatures of standard vs. low-e triple-glazed windows in July 2023.

The results across Figs. 11-14 demonstrate the thermal benefits of using low-e glass in triple-glazed windows. In Fig. 11, the Lower external surface temperature of TG2 compared to TG1 highlights the low-e coating's ability to reflect infrared radiation, reducing heat absorption on the outer pane. Figs. 12 and 13 show that the temperatures in both outer and inner cavities of TG2 remain lower, thanks to the low-e glass's insulating effect, which limits heat transfer into the cavities, especially during peak solar radiation. Finally, Fig. 14 indicates that TG2's internal surface temperature is approximately 4°C lower than TG1's, showing how low-e glass minimizes thermal load on indoor surfaces, enhancing comfort and lowering cooling needs. This performance is due to the low-e layer reflecting incoming heat, reducing heat transmission through the glass, and maintaining a cooler internal environment.

5. Conclusion

The evaluation focused on analyzing the impact of triple-glazed windows on energy efficiency and thermal comfort, emphasizing assessing their thermal performance and understanding the influence of glass optical parameters, particularly low-e glass, to enhance summer comfort. A key finding was that using low-e glass as an insulator significantly reduced the internal surface temperature of TG1. In July, when solar radiation reached 650 W/m², the inner surface temperature of the TG1 embedded with low-e glass (TG2) was 4°C (10.9%) lower than that of TG1 without low-e glass. This demonstrates the superior insulating property of low-e glass in mitigating heat transfer. Moreover, TG2 combined with low-e glass showed the best thermal performance under identical external conditions, as the low-e glass effectively reflected a substantial portion of infrared radiation, reducing the thermal load on interior surfaces. These findings highlight the thermal advantages of integrating low-e glass in triple-glazed window systems, providing valuable insights for enhancing building energy efficiency in hot climates.

Acknowledgements

The authors state that they have no competing financial interests or personal relationships that could have influenced the work presented in this paper

Abbreviations

aw, ae, an, as, ab, at	Coefficients in Finite-Volume equations
dg	glass density
dt	time step
dx, dy, dz	grid spacing
e	Enthalpy
k, j, i	position in the (z, y, x directions)
kg	thermal conductivity of glass (W/m °C)
l	Liquid

N	grid P's North neighbor
NVDSF	Naturally Ventilated Double-Skin Façade
P	Grid point
PCM	Phase Change Materials.
q	Heat generation (W/m ³)
S	Solid
S	'South' in grid P
t	Control-volume face
T	'Top' in grid P
t	Time(s)
T	Temperature (°C)
TG1	Triple glass window with normal glass.
TG2	Triple glass window with low-e glass.
VO2	Vanadium Dioxide.
W	grid P's 'West' neighbor
w	Face of control volume between W and P
z, y, x	Coordinate grid system (m)

Conflict of interest

The authors declare that there are no conflicts of interest regarding the publication of this manuscript.

Author Contribution Statement

Mina A. Nsaif, Jalal M. Jalil, and Mounir Baccar performed the experimental and numerical work.

Mina A. Nsaif, Jalal M. Jalil, and Mounir Baccar proposed the research problem and discussed the results.

Jalal M. Jalil and Mounir Baccar supervised and developed the theory.

References

- [1] M. Kamalisarvestani, R. Saidur, S. Mekhilef, and F. S. Javadi, "Performance, materials and coating technologies of thermochromic thin films on smart windows," *Renewable and Sustainable Energy Reviews*, vol. 26, pp. 353–364, 2013. doi: <https://doi.org/10.1016/j.rser.2013.05.038>.
- [2] K. Khaled and U. Berardi, "Current and future coating technologies for architectural glazing applications," *Energy and Buildings*, vol. 244, p. 111022, 2021. doi: <https://doi.org/10.1016/j.enbuild.2021.111022>.
- [3] L. Long and H. Ye, "Discussion of the performance improvement of thermochromic smart glazing applied in passive buildings," *Solar Energy*, vol. 107, pp. 236–244, 2014. doi: <https://doi.org/10.1016/j.solener.2014.05.014>.
- [4] M. Arnesano et al., "Optimization of the thermochromic glazing design for curtain wall buildings based on experimental measurements and dynamic simulation," *Solar Energy*, vol. 216, pp. 14–25, 2021. doi: <https://doi.org/10.1016/j.solener.2021.01.013>.
- [5] X. Hong et al., "Multi-objective optimization of thermochromic glazing based on daylight and energy performance evaluation," *Building*

- Simulation, vol. 14, pp. 1685–1695, 2021. doi: <https://doi.org/10.1007/s12273-021-0778-7>.
- [6] C. Liu et al., "Index-tunable anti-reflection coatings: Maximizing solar modulation ability for vanadium dioxide-based smart thermochromic glazing," *Journal of Alloys and Compounds*, vol. 731, pp. 1197–1207, 2018. doi: <https://doi.org/10.1016/j.jallcom.2017.10.045>.
- [7] M. Salamati et al., "Daylight performance analysis of TiO₂@W-VO₂ thermochromic smart glazing in office buildings," *Building and Environment*, vol. 186, p. 107351, 2020. doi: <https://doi.org/10.1016/j.buildenv.2020.107351>.
- [8] E. Gagaoudakis et al., "Sputtered VO₂ coatings on commercial glass substrates for smart glazing applications," *Solar Energy Materials and Solar Cells*, vol. 220, p. 110845, 2021. doi: <https://doi.org/10.1016/j.solmat.2020.110845>.
- [9] S. Huang et al., "Determination of optical constants of functional layer of online Low-E glass based on the Drude theory," *Thin Solid Films*, vol. 516, pp. 3179–3183, 2008. doi: <https://doi.org/10.1016/j.tsf.2007.08.137>.
- [10] Z. Yuxuan et al., "Energy saving performance of thermochromic coatings with different colors for buildings," *Energy and Buildings*, vol. 215, p. 109920, 2020. doi: <https://doi.org/10.1016/j.enbuild.2020.109920>.
- [11] Y. Tao et al., "Ventilation performance of a naturally ventilated double skin façade with low-e glazing," *Energy*, vol. 229, p. 120706, 2021. doi: <https://doi.org/10.1016/j.energy.2021.120706>.
- [12] G. Wang et al., "Thermal performance of a novel double-glazed window combining PCM and solar control glass in summer," *Renewable Energy*, vol. 219, p. 119363, 2023. doi: <https://doi.org/10.1016/j.renene.2023.119363>.
- [13] G. Baldinelli, "Double skin façades for warm climate regions: Analysis of a solution with an integrated movable shading system," *Building and Environment*, vol. 44, pp. 1107–1118, 2009. doi: <https://doi.org/10.1016/j.buildenv.2008.08.005>.
- [14] J. M. Jalil and S. M. Salih, "Analysis of Thermal and Insulation Performance of Double-Glazed Window Doped with Paraffin Wax," *Engineering and Technology Journal*, vol. 38, pp. 383–393, 2020. doi: <https://doi.org/10.30684/etj.v38i3A.448>.
- [15] J. M. Jalil and S. M. Salih, "Experimental and numerical investigation of paraffin wax as thermal insulator in a double-glazed window," *Journal of Energy Storage*, vol. 35, p. 102173, 2021. doi: <https://doi.org/10.1016/j.est.2020.102173>.
- [16] B. L. Gowreesunker et al., "Experimental and numerical investigations of the optical and thermal aspects of a PCM-glazed unit," *Energy and Buildings*, vol. 61, pp. 239–249, 2013. doi: <https://doi.org/10.1016/j.enbuild.2013.02.032>.
- [17] X. Yang et al., "Comprehensive performance evaluation of double-glazed windows containing hybrid nanoparticle-enhanced phase change material," *Applied Thermal Engineering*, vol. 223, p. 119976, 2023. doi: <https://doi.org/10.1016/j.applthermaleng.2023.119976>.
- [18] X. Zhang et al., "Performance evaluation of a novel rotatable dynamic window integrated with a phase change material and a vacuum layer," *Energy Conversion and Management*, vol. 272, p. 116333, 2022. doi: <https://doi.org/10.1016/j.enconman.2022.116333>.
- [19] M. Nur-E-Alam et al., "Design, fabrication, and physical properties analysis of laminated Low-E coated glass for retrofit window solutions," *Energy and Buildings*, vol. 318, p. 114427, 2024. doi: <https://doi.org/10.1016/j.enbuild.2024.114427>.
- [20] L. Bianco et al., "Responsive glazing systems: Characterisation methods and winter performance," *Solar Energy*, vol. 155, pp. 372–387, 2017. doi: <https://doi.org/10.1016/j.solener.2017.06.029>.
- [21] L. Bianco et al., "Responsive glazing systems: Characterisation methods, summer performance and implications on thermal comfort," *Solar Energy*, vol. 158, pp. 819–836, 2017. doi: <https://doi.org/10.1016/j.solener.2017.09.050>.
- [22] T. Kułakowski, A. Węglarz, and D. Heim, "An optimisation study of PCM triple glazing for temperate climatic conditions – Dynamic analysis of thermal performance," *Energy*, vol. 283, p. 128361, 2023. doi: <https://doi.org/10.1016/j.energy.2023.128361>.
- [23] H. S. Dheyab and M. Al-Jethelah, "Closed Solar Air Heater System Integrated with PCM RT42 and RT50 in a Thermal Storage-Finned Heat Exchanger Unit," *Tikrit Journal of Engineering Sciences*, vol. 30, pp. 27–37, 2023. doi: <https://doi.org/10.25130/tjes.30.3.4>.
- [24] E. F. Abbas and Sh. A. Azat, "The impact of width of the air gap channel on the mass flow rate, Rayleigh number, and efficiency of passive solar heating system," *Tikrit Journal of Engineering Sciences*, vol. 25, pp. 47–52, 2018. doi: <https://doi.org/10.25130/tjes.25.3.08>.
- [25] K. A. R. Ismail and J. R. Henriquez, "Thermally effective windows with moving phase change material curtains," *Applied Thermal Engineering*, vol. 21, pp. 1909–1923, 2001. doi: <https://doi.org/10.1016/S1359-43110100058-8>.
- [26] K. A. R. Ismail and J. R. Henriquez, "PCM glazing systems," *International Journal of Energy Research*, vol. 21, pp. 1241–1255, 1997.
- [27] K. A. R. Ismail, C. T. Salinas, and J. R. Henriquez, "Comparison between PCM filled glass windows and absorbing gas filled windows," *Energy and Buildings*, vol. 40, pp. 710–719, 2008. doi: <https://doi.org/10.1016/j.enbuild.2007.05.005>.
- [28] E. Sorooshnia et al., "A novel approach for optimized design of low-E windows and visual comfort for residential spaces," *Energy and Built Environment*, 2023. doi: <https://doi.org/10.1016/j.enbenv.2023.08.002>.
- [29] F. Goia, M. Perino, and M. Haase, "A numerical model to evaluate the thermal behaviour of PCM glazing system configurations," *Energy and Buildings*, vol. 54, pp. 141–153, 2012. doi: <https://doi.org/10.1016/j.enbuild.2012.07.036>.
- [30] F. Goia, "Thermo-physical behaviour and energy performance assessment of PCM glazing system configurations: a numerical analysis," *Frontiers of Architectural Research*, vol. 1, pp. 341–347, 2012. doi: <https://doi.org/10.1016/j.foar.2012.10.002>.
- [31] F. Goia, M. Perino, and V. Serra, "Improving thermal comfort conditions by means of PCM glazing systems," *Energy and Buildings*, vol. 60, pp. 442–452, 2013. doi: <https://doi.org/10.1016/j.enbuild.2013.01.029>.
- [32] F. Goia, M. Perino, and V. Serra, "Experimental analysis of the energy performance of a full-scale PCM glazing prototype," *Solar Energy*, vol. 100, pp. 217–233, 2014. doi: <https://doi.org/10.1016/j.solener.2013.12.002>.
- [33] H. Koshlak et al., "Experimental and numerical studies of heat transfer through a double-glazed window with electric heating of the glass surface," *Sustainability*, vol. 16, no. 21, p. 9374, 2024. doi: <https://doi.org/10.3390/su16219374>.
- [34] B. Basok et al., "Comprehensive investigation of the thermal performance of an electrically heated double-glazed window: A theoretical and experimental approach," *Energies*, vol. 17, no. 44, p. 4491, 2024. doi: <https://doi.org/10.3390/en17174491>.
- [35] Z. Respondek, "Climatic loads on triple-glazed insulating glass units used as an external horizontal building envelope," in *Proceedings of CEE 2023, Lecture Notes in Civil Engineering*, vol. 438, pp. 1–12, 2023. doi: https://doi.org/10.1007/978-3-031-44955-0_33.
- [36] X. Wang et al., "Modeling, simulation, and performance analysis of a liquid-infill tunable window," *Sustainability*, vol. 14, no. 23, p. 15968, 2022. doi: <https://doi.org/10.3390/su142315968>.
- [37] Sh. Li et al., "Experimental research on the dynamic thermal performance of a novel triple-pane building window filled with PCM," *Sustainable Cities and Society*, vol. 27, pp. 15–22, 2016. doi: <https://doi.org/10.1016/j.scs.2016.08.014>.